Synthesis, structures and magnetic behaviour of new anionic copper(II) sulfate aggregates and chains

Andrew D. Burrows,[a]* Mary F. Mahon,[a] Viorica M. Sebestyen,[a] Yanhua Lan[b] and Annie K. Powell[b,c]

[a] Department of Chemistry, University of Bath, Claverton Down, Bath BA2 7AY, UK.

[b] Institut für Anorganische Chemie, Karlsruhe Institute of Technology, Engesserstrasse 15, D76131 Karlsruhe, Germany.

[c] Institute of Nanotechnology, Karlsruhe Institute of Technology, Hermann-von-Helmholtz Platz 1, 76344 Eggenstein-Leopoldshafen, Germany.

Abstract

The reaction between $CuSO_4 \cdot 5H_2O$ and $[NMe_2H_2]Cl$ in DMF at 95 °C yielded green crystals of $(NMe_2H_2)_4[Cu_6O_2(SO_4)_6(DMF)_4]$ **1**. The discrete $[Cu_6(\mu_4\text{-}O)_2(\mu_3\text{-}SO_4)_4(\mu_2\text{-}SO_4)_2(DMF)_4]^{4-}$ anions present in **1** contain two edge-sharing $Cu_4(\mu_4\text{-}O)$ tetrahedra, with the copper(II) centres bridged by sulfato ligands. These anions are linked into a two-dimensional network through hydrogen bonds involving the dimethylammonium cations. When the reaction was carried out in the absence of $[NMe_2H_2]Cl$, yellow-green crystals of $(NMe_2H_2)_4[Cu_6O_2(SO_4)_6(DMF)_2]$ **2** were obtained. The anions in **2** contain similar $Cu_6O_2(SO_4)_6$ aggregates to those in **1**, though these differ in terms of the copper(II) coordination geometries. In addition, the anions in **2** are linked into chains through bridging sulfato ligands. The $Cu_6O_2(SO_4)_6$ aggregates observed in **1** and **2** are related to those present in the rare copper sulfate mineral fedotovite, $K_2Cu_3O(SO_4)_3$, and in common with this mineral both **1** and **2** decompose in the presence of moisture. The reaction between $CuSO_4 \cdot 5H_2O$ and $[NMe_2H_2]Cl$ in DMF at room temperature gave $(NMe_2H_2)[Cu_2(OH)(SO_4)_2(H_2O)_2]$ **3**, the structure of which contains triangular $Cu_3(OH)(SO_4)$ units that share vertices to form tapes. Magnetic measurements revealed that **1** and **3** are both spin-canting metamagnetic systems. Field-induced responses were observed below 5 K, with the critical field indicating metamagnetic behaviour from antiferromagnetic to ferromagnetic equal to 110 Oe for both compounds.

Introduction

Copper(II) sulfate is one of the first compounds encountered by many budding chemists, with the distinctive blue colour of the pentahydrate readily recognisable. It is used in a wide range of school experiments including crystal growing, dehydration and copper plating. Copper(II) sulfate also has many industrial applications including use as a fungicide, algaecide and molluscicide,[1-3] and as an activator in the concentration by froth flotation in the mining industry.[4] A wide variety of copper(II) sulfate minerals are also known in which the copper(II) and sulfate ions occur together with anions such as hydroxide,[5,6] or cations such as sodium or potassium.[7]

Copper(II) sulfate is often used in combination with multidentate *N*-donor ligands to form coordination networks. Since sulfate is generally a better ligand than nitrate or perchlorate, reactions with $CuSO_4 \cdot 5H_2O$ are more likely to lead to mixed-ligand products than analogous reactions with $Cu(NO_3)_2$ or $Cu(ClO_4)_2$. For example, reactions of $CuSO_4 \cdot 5H_2O$ with pyridine-substituted tetrazoles were recently reported to lead to open framework coordination networks containing both sulfate and pyridyl-tetrazolate ligands,[8] whereas reactions involving chelating ligands have afforded sulfate-bridged dimers.[9] Sulfates can link copper(II) centres into aggregates such as hexamers[10] and tetramers,[11] that can themselves be further cross-linked into extended structures. Coordination networks can even be formed in the absence of additional ligands, and a number of anionic copper(II) sulfate structures have been reported in which the charges on the anions are balanced by included ammonium cations.[12]

In this paper we report the synthesis and characterisation of three new copper(II) sulfate compounds, in which anionic copper-sulfate aggregates and chains are charge balanced by dimethylammonium ions derived either from the hydrolysis of the *N*,*N*′-dimethylformamide (DMF) solvent[13] or from the addition of $[NMe_2H_2]Cl$. These compounds have been crystallographically characterised as $(NMe_2H_2)_4[Cu_6O_2(SO_4)_6(DMF)_4]$ **1**,

$(NMe_2H_2)_4[Cu_6O_2(SO_4)_6(DMF)_2]$ **2** and $(NMe_2H_2)[Cu_2(OH)(SO_4)_2(H_2O)_2]$ **3**, and the magnetic properties of **1** and **3** have also been investigated.

Experimental Section

General

The reagents used for the syntheses were purchased commercially and used without further purification. The DMF was ACS reagent quality.

Powder X-ray diffraction patterns were recorded on a Bruker AXS D8 Advance diffractometer with copper Kα radiation of wavelength 1.5406 Å at 298 K. DMF-saturated samples were placed in 0.5 mm diameter Lindemann capillaries, and measured with a 2θ range of 3-60°. The step size was 0.016° with a time per step of 134.5 s. Simulated X-ray powder patterns were generated from single crystal data that were imported into PowderCell,[14] with the step size of 0.02° and time per step of 1.00 s.

Magnetic susceptibility measurements were obtained using a Quantum Design SQUID (superconducting quantum interference device) MPMS-XL susceptometer. This magnetometer works between 1.8 and 400 K for direct current (DC) applied fields ranging from –70 to 70 kOe. Measurements were performed on polycrystalline samples of **1** (33.0 mg) and **3** (36.7 mg). Alternating current (AC) susceptibility measurements were measured with an oscillating AC field of 3Oe and AC frequencies at 1000 Hz. The magnetic data were corrected for the sample holder.

Synthesis of $(NMe_2H_2)_4[Cu_6O_2(SO_4)_6(DMF)_4]$ 1

$CuSO_4 \cdot 5H_2O$ (0.060 g, 0.24 mmol) and $[NMe_2H_2]Cl$ (0.013 g, 0.16 mmol) were dissolved with stirring in DMF (12 cm^3). The reaction mixture was placed in a 30 cm^3 thick-walled glass vial and heated at 95°C for 24 h to yield tiny green crystals. The PXRD pattern of the product showed a good match with the pattern simulated from the X-ray single crystal

structure (Fig. S1). The sample was carefully dried under a flow of nitrogen and stored in a sealed flask under nitrogen.

Synthesis of $(NMe_2H_2)_4[Cu_6O_2(SO_4)_6(DMF)_2]$ 2

$CuSO_4 \cdot 5H_2O$ (0.60 g, 2.4 mmol) was dissolved with stirring in DMF (12 cm^3). This solution was placed in a 30 cm^3 thick-walled glass vial and heated at 95°C for 24 h. The powder X-ray diffraction pattern of the resultant tiny yellow-green crystals matches that simulated from the X-ray crystal structure (Fig. S2). The sample was carefully dried under a flow of nitrogen and stored in a sealed flask under nitrogen.

Synthesis of $(NMe_2H_2)[Cu_2(OH)(SO_4)_2(H_2O)_2]$ 3

$CuSO_4 \cdot 5H_2O$ (0.6 g, 2.4 mmol) and $[NMe_2H_2]Cl$ (0.13 g, 1.6 mmol) were dissolved with stirring in DMF (12 cm^3). This solution was placed in a vial and left undisturbed at room temperature. Turquoise crystals started to appear after a week, but the crystals were left in the mother liquor for a further two weeks after which they were harvested. The powder X-ray diffraction pattern of the product matches that simulated from the X-ray crystal structure (Fig. S3).

X-ray crystallography

X-ray diffraction data on structures were collected on a Nonius Kappa CCD diffractometer, using Mo-Kα radiation of wavelength 0.71073 Å at 150 K. Crystal data and details of the structural refinements are given in Table 1. The structures were solved using SHELXS-97 and refined using full-matrix least squares in SHELXL-97.[15] The final refinements were generally straightforward. Unless noted below, all non-hydrogen atoms were refined anisotropically in the final least squares run, and hydrogen atoms were included at calculated positions. In the structure of **2**, one of the dimethylammonium cations (that based on N(3)), was disordered in a 80:20 ratio. Only the major occupancy fragment atoms therein were refined anisotropically. Oxygen bound hydrogen atoms for **3** were located and refined at

0.98 Å from the relevant parent atoms, whereas in **1-3** nitrogen bound hydrogen atoms were located and refined at 0.92 Å from the relevant parent atoms.

Table 1 – Crystal data and structure refinement details for compounds **1-3**.

Compound	**1**	**2**	**3**
Chemical formula	$C_{20}H_{60}Cu_6N_8O_{30}S_6$	$C_{14}H_{46}Cu_6N_6O_{28}S_6$	$C_2H_{13}Cu_2NO_{11}S_2$
M	1466.36	1320.17	418.33
Crystal system	Monoclinic	Triclinic	Monoclinic
Space group	$P2_1/n$	$P\bar{1}$	$P2_1/n$
a/Å	13.1050(3)	8.5880(2)	6.8990(1)
b/Å	10.5140(2)	10.6840(3)	17.0780(4)
c/Å	18.7530(5)	12.8170(3)	10.3860(3)
α/°	90.00	106.496(1)	90.00
β/°	103.183(1)	104.593(1)	90.779(1)
γ/°	90.00	105.935(2)	90.00
Unit cell volume/Å^3	2515.81(10)	1012.49(4)	1223.58(5)
Temperature/K	150(2)	150(2)	150(2)
Z	2	1	4
No. of reflections measured	39253	15974	22218
No. of independent reflections	5766	4615	2802
R_{int}	0.1191	0.0492	0.0879
Final R_1 values ($I > 2\sigma(I)$)	0.0582	0.0326	0.0389
Final $wR(F^2)$ values ($I > 2\sigma(I)$)	0.1230	0.0760	0.0811
Final R_1 values (all data)	0.0890	0.0450	0.0636
Final $wR(F^2)$ values (all data)	0.1379	0.0813	0.0910
Goodness of fit on F^2	1.077	1.068	1.069

Results and Discussion

Compounds **1** and **2** were initially obtained serendipitously from reaction mixtures containing copper(II) sulfate pentahydrate and dicarboxylic acids in DMF, though subsequently the presence of the dicarboxylic acid was found to be unnecessary. Compound **1** was prepared by heating a mixture of $CuSO_4 \cdot 5H_2O$ and $[NMe_2H_2]Cl$ in DMF at 95 °C for 24 hours. Powder X-ray diffraction studies on the resulting tiny green crystals revealed that **1** is metastable, with the compound undergoing a series of structural changes over the course of a month. Compound **2** was prepared as tiny yellow-green crystals by heating $CuSO_4 \cdot 5H_2O$ in DMF at 95 °C for 24 hours. As with **1**, compound **2** is metastable, undergoing a series of structural changes over several weeks, as witnessed by changes in the powder X-ray diffraction patterns. When water was added to the DMF solvent, the reaction gave a turquoise solid that was

shown by powder X-ray diffraction to be $Cu_3(SO_4)(OH)_4$, which is the mineral antlerite.[16] Compound **3** was prepared from a mixture of $CuSO_4 \cdot 5H_2O$ and $[NMe_2H_2]Cl$ in DMF at room temperature, with the resultant turquoise crystals harvested after three weeks.

Compounds **1-3** are all moisture-sensitive, with **1** and **2** decomposing rapidly in the presence of water and **3** decomposing more slowly. These decompositions occur with absorption of water to form pastes and colour changes to pale blue. The sensitivity of **1-3** prevented accurate microanalysis from being obtained, though in all cases the powder X-ray diffraction patterns of the DMF-saturated samples (Figures S1-S3) show a good correspondence to those simulated from the X-ray single crystal analyses (*vide infra*).

The crystal structure of $(NMe_2H_2)_4[Cu_6O_2(SO_4)_6(DMF)_4]$ **1** contains dimethylammonium cations and discrete $[Cu_6O_2(SO_4)_6(DMF)_4]^{4-}$ anions. The anions contain two edge-sharing $Cu_4(\mu_4\text{-}O)$ tetrahedra (Fig. 1a), with the four triangular Cu_3 faces not involving the shared edge each capped by a μ_3-sulfato ligand. Two μ_2-sulfato ligands bridge between pairs of non-shared vertices on the two tetrahedra, and each copper centre not involved in edge-sharing is also coordinated to a DMF ligand (Fig. 1b). Hence the anion can be represented as $[Cu_6(\mu_4\text{-}O)_2(\mu_3\text{-}SO_4)_4(\mu_2\text{-}SO_4)_2(DMF)_4]^{4-}$. Selected bond lengths and angles for **1** are presented in Table 2. The $Cu_6O_2(SO_4)_6$ core is unusual, with the only previous example observed in the mineral fedotovite (*vide infra*).

Table 2. Selected bond lengths (Å) and bond angles (°) for **1**. Primed atoms generated by the symmetry operation $-x + 2, -y, -z$.

Cu(1)-O(1)'	1.937(3)	Cu(1)-O(2)	1.946(4)
Cu(1)-O(1)	1.949(3)	Cu(1)-O(6)'	1.972(4)
Cu(2)-O(3)	1.966(5)	Cu(2)-O(1)	1.943(3)
Cu(2)-O(7)	2.029(4)	Cu(2)-O(14)	1.988(5)
Cu(3)-O(1)	1.931(3)	Cu(2)-O(11)'	2.127(4)
Cu(3)-O(15)	1.972(4)	Cu(3)-O(4)	1.961(5)
Cu(3)-O(10)	2.114(4)	Cu(3)-O(8)	2.107(4)
O(1)'-Cu(1)-O(2)	173.55(16)	O(1)'-Cu(1)-O(1)	86.08(14)
O(2)-Cu(1)-O(1)	93.59(16)	O(1)'-Cu(1)-O(6)'	96.46(15)
O(2)-Cu(1)-O(6)'	83.63(17)	O(1)-Cu(1)-O(6)'	176.64(15)

O(1)-Cu(2)-O(3)	91.71(17)	O(1)-Cu(2)-O(14)	174.55(18)
O(3)-Cu(2)-O(14)	86.6(2)	O(1)-Cu(2)-O(7)	95.27(15)
O(3)-Cu(2)-O(7)	145.7(2)	O(14)-Cu(2)-O(7)	83.29(19)
O(1)-Cu(2)-O(11)'	93.00(15)	O(3)-Cu(2)-O(11)'	119.7(2)
O(14)-Cu(2)-O(11)'	92.33(19)	O(7)-Cu(2)-O(11)'	93.46(18)
O(1)-Cu(3)-O(4)	93.17(17)	O(1)-Cu(3)-O(15)	176.64(16)
O(4)-Cu(3)-O(15)	87.72(18)	O(1)-Cu(3)-O(8)	91.49(14)
O(4)-Cu(3)-O(8)	129.9(2)	O(15)-Cu(3)-O(8)	85.46(16)
O(1)-Cu(3)-O(10)	87.40(15)	O(4)-Cu(3)-O(10)	143.8(2)
O(15)-Cu(3)-O(10)	93.80(17)	O(8)-Cu(3)-O(10)	86.15(16)

The copper(II) centres involved in edge-sharing, Cu(1), have distorted square planar geometries, coordinated to two oxo and two μ_3-sulfato ligands. The Cu(1)–O bond lengths lie between 1.937(3) and 1.972(4) Å, with *cis* O–Cu(1)–O bond angles between 83.63(17) and 96.46(15)°, and the Cu(1) centre lies 0.072 Å from the mean plane defined by the four coordinating oxygen atoms. The Cu(1)···Cu(1)' separation is 2.840(1) Å.

In contrast, Cu(2) and Cu(3), are both five-coordinate, with geometries between those expected for ideal square pyramidal and trigonal bipyramidal structures, as witnessed by τ values of 0.48 and 0.55 respectively.[17] Both of these copper(II) centres are coordinated to an oxo ligand, three sulfato ligands and a DMF molecule. The DMF oxygen atom and oxo ligand are almost co-linear [O(1)–Cu(2)–O(14) 174.55(18)°, O(1)–Cu(3)–O(15) 176.64(16)°], with the three oxygen atoms from the sulfato groups approximately co-planar.

In the crystal structure of **1**, the anions are linked into sheets by hydrogen bonding to the dimethylammonium cations (Fig. 1c). The hydrogen bonds primarily involve the non-coordinated oxygen atoms of the sulfato ligands [O(12), O(13), O(9)] acting as acceptors, though notably the coordinated oxygen atom O(8) acts as an acceptor in place of the non-coordinated atom O(5), presumably for geometrical reasons. There are no strong interactions between the hydrogen-bonded sheets.

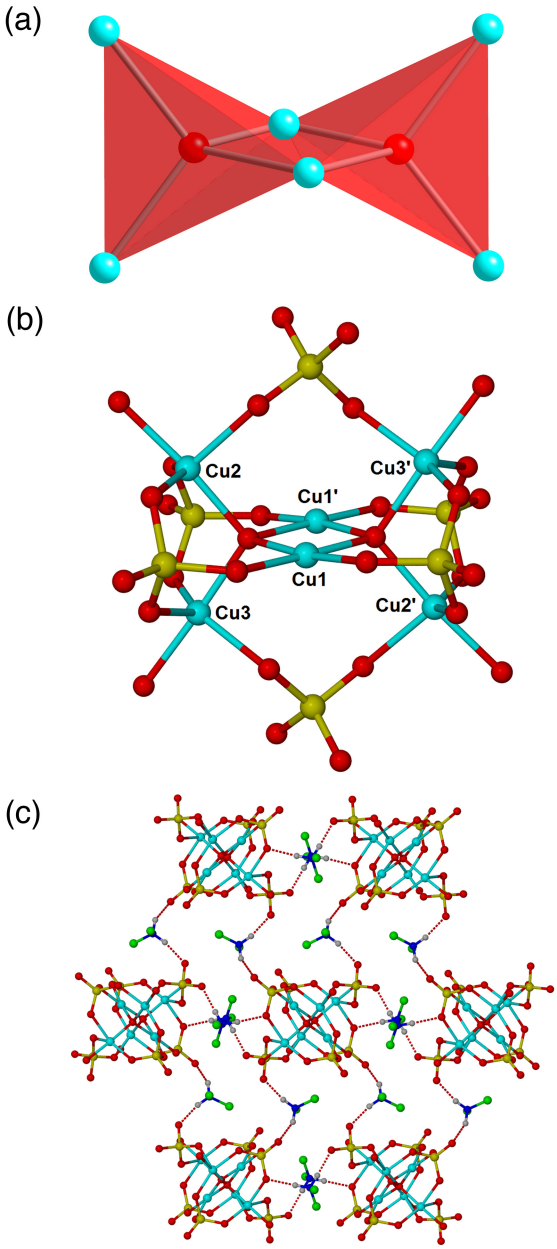

Figure 1. The structure of $(NMe_2H_2)_4[Cu_6O_2(SO_4)_6(DMF)_4]$ **1**, showing (a) the edge-sharing tetrahedra of the central Cu_6 aggregate, (b) the $[Cu_6O_2(SO_4)_6(DMF)_4]^{4-}$ anion, and (c) hydrogen bonding between the dimethylammonium cations and the $[Cu_6O_2(SO_4)_6(DMF)_4]^{4-}$ anions linking the aggregates into sheets. The non-oxygen atoms of the DMF ligands and all hydrogen atoms except those involved in hydrogen bonding have been removed for clarity. Primed atoms are generated by the symmetry operation $-x + 2, -y, -z$.

The crystal structure of $(NMe_2H_2)_4[Cu_6O_2(SO_4)_6(DMF)_2]$ **2** contains dimethylammonium cations and $[Cu_6O_2(SO_4)_6(DMF)_2]^{4-}$ anions. Selected bond lengths and angles are presented in Table 3. The structure of each $[Cu_6O_2(SO_4)_6(DMF)_2]^{4-}$ aggregate is broadly similar to the discrete $[Cu_6O_2(SO_4)_6(DMF)_4]^{4-}$ aggregates in **1** – two edge-sharing $Cu_4(\mu_4\text{-O})$ tetrahedra are bridged by sulfato groups (Fig. 2a). However, there are two significant differences between the aggregates in **1** and **2**. Firstly, in **2**, the copper(II) centres involved in edge-sharing, Cu(1), exhibit square pyramidal geometry, with a τ value of 0.04, in contrast to the equivalent square planar centres in **1**. In **2**, Cu(1) is additionally coordinated to an oxygen atom from the sulfato ligand bridging between the copper(II) centres at the ends of the two tetrahedra. The axial contact – Cu(1)–O(10) 2.214(2) Å – is longer than those in the basal plane [1.952(2) – 1.999(2) Å], but significantly shorter than the analogous non-bonded contact in **1** [Cu(1)···O(10) 2.666(4) Å].

Table 3. Selected bond lengths (Å) and bond angles (°) for **2**. Primed atoms generated by the symmetry operation $-x + 2, -y, -z$. Double primed atoms generated by the symmetry operation $x + 1, y, z$.

Cu(1)-O(1)	1.952(2)	Cu(1)-O(1)'	1.990(2)
Cu(1)-O(2)	1.999(2)	Cu(1)-O(8)'	1.972(2)
Cu(1)-O(10)	2.214(2)	Cu(2)-O(1)	1.9494(19)
Cu(2)-O(3)	2.102(2)	Cu(2)-O(6)	2.021(2)
Cu(2)-O(12)'	2.122(2)	Cu(2)-O(13)"	1.946(2)
Cu(3)-O(1)	1.956(2)	Cu(3)-O(4)	1.985(2)
Cu(3)-O(7)	2.021(2)	Cu(3)-O(11)	2.143(2)
Cu(3)-O(14)	1.991(2)		
O(1)-Cu(1)-O(8)'	169.88(9)	O(1)-Cu(1)-O(1)'	86.99(8)
O(8)'-Cu(1)-O(1)'	94.62(8)	O(1)-Cu(1)-O(2)	94.90(8)
O(8)'-Cu(1)-O(2)	82.22(9)	O(1)'-Cu(1)-O(2)	172.19(8)
O(1)-Cu(1)-O(10)	97.79(8)	O(8)'-Cu(1)-O(10)	92.05(8)
O(1)'-Cu(1)-O(10)	94.47(8)	O(2)-Cu(1)-O(10)	92.78(8)
O(13)"-Cu(2)-O(1)	168.09(9)	O(1)-Cu(2)-O(6)	90.67(8)
O(13)"-Cu(2)-O(6)	85.90(9)	O(1)-Cu(2)-O(3)	93.21(8)
O(13)"-Cu(2)-O(3)	81.94(9)	O(13)"-Cu(2)-O(12)'	92.62(9)
O(6)-Cu(2)-O(3)	138.44(9)	O(6)-Cu(2)-O(12)'	121.35(8)
O(1)-Cu(2)-O(12)'	98.89(8)	O(3)-Cu(2)-O(12)'	98.86(9)
O(1)-Cu(3)-O(4)	94.78(9)	O(1)-Cu(3)-O(14)	171.96(9)
O(4)-Cu(3)-O(14)	82.64(9)	O(1)-Cu(3)-O(7)	94.10(8)
O(4)-Cu(3)-O(7)	146.40(10)	O(14)-Cu(3)-O(7)	84.09(9)
O(1)-Cu(3)-O(11)	100.90(8)	O(4)-Cu(3)-O(11)	110.28(9)
O(14)-Cu(3)-O(11)	87.13(9)	O(7)-Cu(3)-O(11)	99.69(9)

The second significant change involves the number of coordinated DMF molecules. In **2** there are only two DMF ligands per anion, so Cu(2) is not solvated. Instead, it forms a Cu–O bond to a sulfato ligand from a neighbouring aggregate [Cu(2)–O(13) 1.946(2) Å]. These interactions occur pairwise, and link the aggregates into chains that run along the *a* axis (Fig. 2b). The coordination geometries of Cu(2) and Cu(3) are broadly similar to those of the equivalent atoms in **1**, being between those expected for ideal square pyramidal and trigonal bipyramidal geometries, as witnessed by τ values of 0.49 and 0.43 respectively. A consequence of these changes is that the μ_2-sulfato ligand in **1** is replaced by a μ_4-sulfato ligand in **2**.

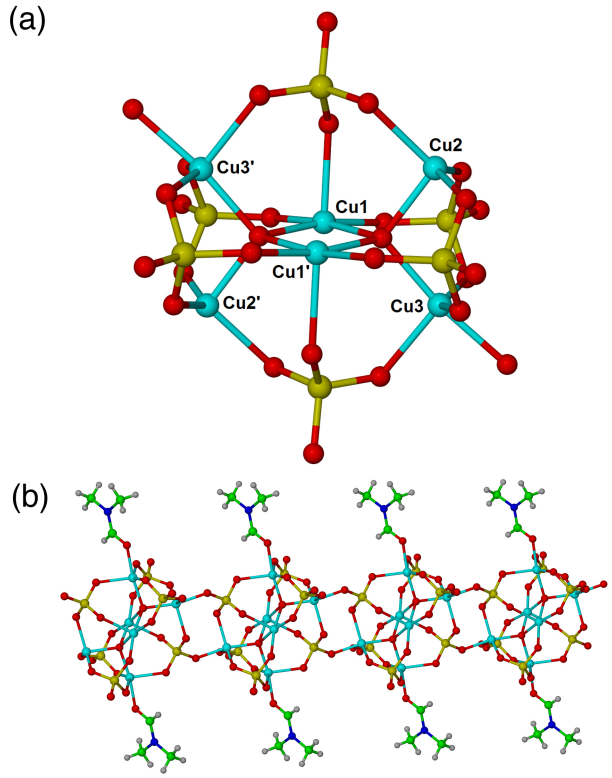

Figure 2. The structure of $(NMe_2H_2)_4[Cu_6O_2(SO_4)_6(DMF)_2]$ **2**, showing (a) the $[Cu_6O_2(SO_4)_6(DMF)_4]^{4-}$ anion, with the non-oxygen atoms of the DMF ligands removed for clarity, and (b) linking of the $[Cu_6O_2(SO_4)_6(DMF)_4]^{4-}$ aggregates into chains. Primed atoms are generated by the symmetry operation $-x + 2, -y, -z$.

As with **1**, hydrogen bonds are observed between the NH groups of the dimethylammonium cations and the sulfato oxygen atoms, with non-coordinated atoms O(5) and O(9) acting as hydrogen bond acceptors along with coordinated oxygen atoms O(6) and O(12). These

hydrogen bonds link the one-dimensional coordination polymers into a three-dimensional network.

The crystal structures of **1** and **2** both have features in common with the structure of the rare copper sulfate mineral fedotovite, $K_2Cu_3O(SO_4)_3$,[18] which was first observed as a sublimate from the Tolbachik volcanic eruption in Kamchatka, Russia. Fedotovite contains the only previously reported example of the same $[Cu_6(\mu_4\text{-}O)_2(\mu_3\text{-}SO_4)_4(\mu_2\text{-}SO_4)_2]^{4-}$ building blocks (Fig. 3a) as in **1**, though the μ_2-sulfato groups bridge between these aggregates to form a two-dimensional coordination network (Fig. 3b), which is linked into a three-dimensional structure by the potassium ions. Notably, like **1** and **2**, fedotovite has been observed to be unstable in air.

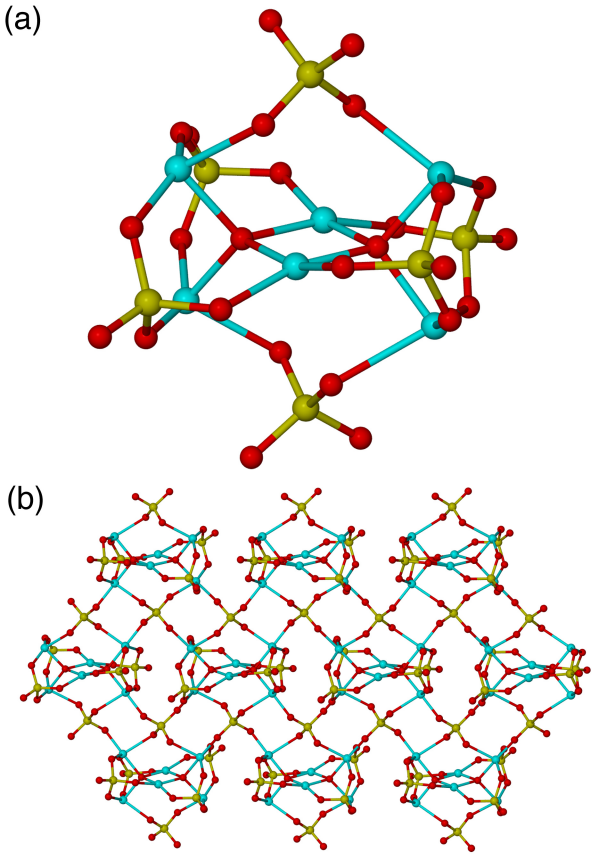

Figure 3. The structure of $K_2Cu_3O(SO_4)_3$, fedotovite, showing (a) the $Cu_6O_2(SO_4)_6$ aggregates, and (b) linking of the aggregates into sheets. Potassium cations have been removed for clarity.

The crystal structure of $(NMe_2H_2)[Cu_2(OH)(SO_4)_2(H_2O)_2]$ **3** reveals a different solid-state architecture to those observed for **1** and **2**. In particular, **3** consists of triangular $Cu_3(\mu_3\text{-}OH)(\mu_3\text{-}SO_4)$ units that share vertices to form tapes running along the crystallographic *a* axis (Fig. 4a). These tapes are reinforced by $\mu_4\text{-}SO_4$ ligands (Fig. 4b). Selected bond lengths and angles for **3** are presented in Table 4.

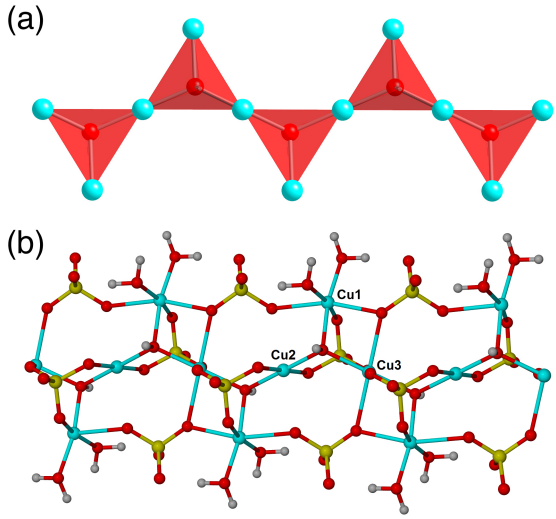

Figure 4. The structure of $(NMe_2H_2)[Cu_2(OH)(SO_4)_2(H_2O)_2]$ **3**, showing (a) the linked $Cu_3(OH)$ triangles, and (b) the $[Cu_2(OH)(SO_4)_2(H_2O)_2]^-$ tapes.

Table 4. Selected bond lengths (Å) and bond angles (°) for **3**. Primed atoms generated by the symmetry operation $x + 1, y, z$. Double primed generated by the symmetry operation $-x, -y + 2, -z + 2$. Triple primed generated by the symmetry operation $-x + 1, -y + 2, -z + 2$.

Cu(1)-O(10)	1.970(3)	Cu(1)-O(6)	1.984(3)
Cu(1)-O(11)	1.985(3)	Cu(1)-O(1)	2.012(3)
Cu(1)-O(5)'	2.281(3)	Cu(1)-O(2)	2.384(3)
Cu(2)-O(1)	1.941(3)	Cu(2)-O(7)	1.960(3)
Cu(3)-O(1)	2.019(3)	Cu(3)-O(5)'	2.377(3)
Cu(3)-O(8)	1.932(3)		
O(10)-Cu(1)-O(6)	86.65(12)	O(10)-Cu(1)-O(11)	95.92(12)
O(6)-Cu(1)-O(11)	166.99(12)	O(10)-Cu(1)-O(1)	169.40(12)
O(6)-Cu(1)-O(1)	91.00(11)	O(11)-Cu(1)-O(1)	88.69(12)
O(10)-Cu(1)-O(5)'	90.85(11)	O(6)-Cu(1)-O(5)'	94.08(12)
O(11)-Cu(1)-O(5)'	98.62(12)	O(1)-Cu(1)-O(5)'	79.00(10)
O(10)-Cu(1)-O(2)	103.81(11)	O(6)-Cu(1)-O(2)	80.10(11)
O(11)-Cu(1)-O(2)	86.90(11)	O(1)-Cu(1)-O(2)	85.93(10)
O(5)'-Cu(1)-O(2)	163.78(10)	O(1)-Cu(2)-O(7)	90.84(12)
O(1)''-Cu(2)-O(7)	89.16(12)	O(8)-Cu(3)-O(1)	92.33(11)
O(8)-Cu(3)-O(1)'''	87.67(11)	O(8)-Cu(3)-O(5)''	86.42(11)
O(1)-Cu(3)-O(5)''	103.40(10)	O(8)-Cu(3)-O(5)'	93.58(11)

O(1)-Cu(3)-O(5)'	76.60(10)		

The copper(II) centres Cu(2) and Cu(3) link the triangles together into the tapes. These both exhibit tetragonally distorted octahedral geometries, and are coordinated to two hydroxyl oxygen atoms and two μ_3-sulfato oxygen atoms in the equatorial plane, with two longer contacts to the μ_4-sulfato oxygen atoms in the axial positions. The copper(II) centre Cu(1) also has a tetragonally distorted octahedral geometry, and is coordinated to a hydroxyl group, two aqua ligands and a μ_3-sulfato oxygen atom in the equatorial plane, and to two μ_4-sulfato oxygen atoms in the axial positions.

The tapes are supported by the presence of intramolecular hydrogen bonds between the coordinated aqua ligands and the non-coordinated oxygen atoms of the μ_4-sulfate [O(11)···O(3) 2.682, H(11A)···O(3) 1.76 Å, O(11)–H(11A)···O(3) 157°; O(10)···O(4) 2.754, H(10B)···O(4) 1.78 Å, O(10)–H(10B)···O(4) 174°]. There are also intermolecular hydrogen bonds between the tapes that involve the aqua ligands [O(11)···O(4) 2.718, H(11B)···O(4) 1.74 Å, O(11)–H(11B)···O(4) 177°; O(10)···O(3) 2.670, H(10A)···O(3) 1.70 Å, O(10)–H(10A)···O(3) 171°] and these link the tapes into sheets. Furthermore, hydrogen bonds are present between the dimethylammonium cations and the coordinated sulfato oxygen atoms, though notably the hydroxyl O–H group does not act as a hydrogen bond donor.

Although triangular $Cu_3(\mu_3\text{-OH})$ building blocks are relatively well-known in both discrete compounds[19] and polymeric arrays,[16] there are only three previously reported examples of compounds containing $Cu_3(\mu_3\text{-OH})(\mu_3\text{-SO}_4)$ units, in which the second face of the triangle is capped by a sulfato ligand. These are a discrete Cu_3 compound that was reported by Beckett and Hoskins in 1972,[20] and two $Cu_{10}(SO_4)_8$ aggregates that were reported more recently.[21,22]

Given the proximity of the $3d^9$ copper(II) centres in **1-3**, their magnetic properties are potentially interesting. In order to explore this, magnetic measurements were undertaken on

compounds **1** and **3**. Plots of magnetic susceptibility χT against temperature for **1** and **3** in an external magnetic field of 1000 Oe are shown in Figures 5a and 6a, respectively. Both compounds display antiferromagnetic interactions at high temperatures, with the greater temperature dependence observed for **1** suggesting stronger antiferromagnetic interactions in this compound. This result is confirmed by a Curie-Weiss fit to the data above 60 K, which leads to Weiss constants (θ) of –82.0 and –18.7 K for **1** and **3**, respectively (Figure S4). Below 20 K (Figs. 5b, 6b) the susceptibility χT increases rapidly and reaches a maximum at a temperature of approximate 3 K. The maximum value of χT increases with the decrease of the external applied magnetic field from 1000 to 100 Oe. This type of field-induced response in the susceptibility is related to the unpaired spins of the d^9 copper(II) centres canting to each other at very low temperatures.

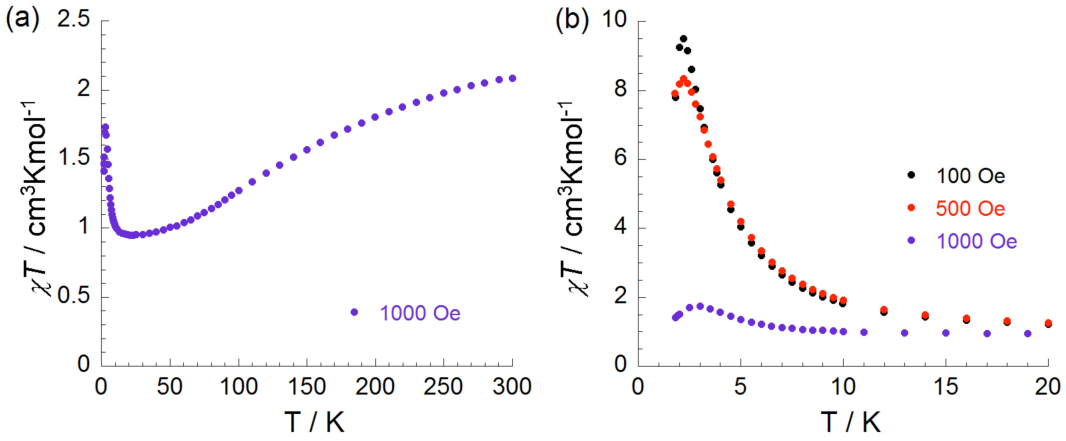

Figure 5. Magnetic susceptibility (χT) *vs.* temperature for $(NMe_2H_2)_4[Cu_6O_2(SO_4)_6(DMF)_4]$ **1** (a) at 1000 Oe and (b) below 20 K for the indicated applied magnetic fields.

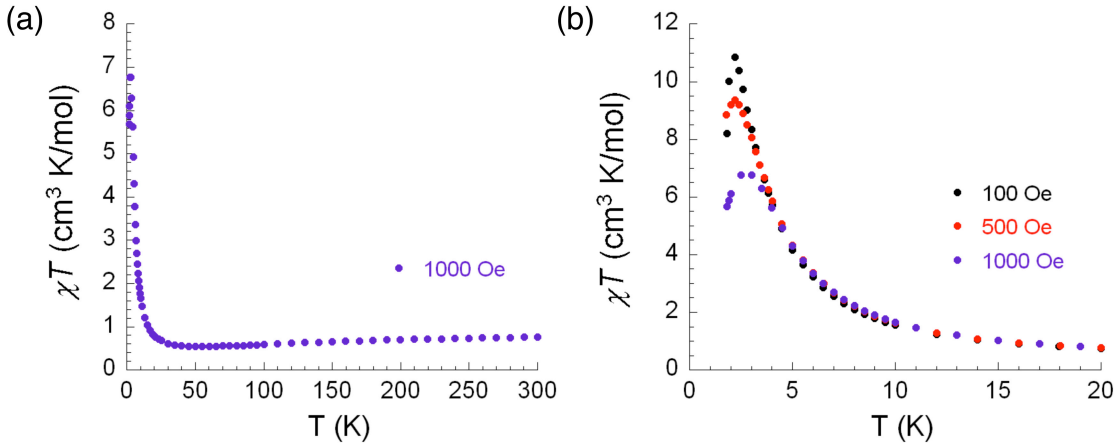

Figure 6. Magnetic susceptibility (χT) *vs.* temperature for $(NMe_2H_2)[Cu_2(OH)(SO_4)_2(H_2O)_2]$ **3** (a) at 1000 Oe and (b) below 20 K for the indicated applied magnetic fields.

Magnetisation curves for **1** and **3** at temperatures below 5 K (Figs. 7a, 8a) reveal that the magnetisation, *M*, increases with the external magnetic field, *H*. For **1**, the magnetisation increases slowly with *H*, reaching approximately 1.2 μB at 70 000 Oe though no saturation point was observed. For **3**, the magnetisation increases more rapidly and almost reaches a saturation of 1.1 μB at 70 000 Oe. Derivative plots of the magnetisation *M* against external magnetic field *H* are shown in Figures 7b and 8b, respectively. In both cases, metamagnetic behaviour is suggested by the presence of an inflection point at a field of 110 Oe, which represents the characteristic field at which the magnetic field overcomes the antiferromagnetic interactions, allowing for parallel alignment of the spins.

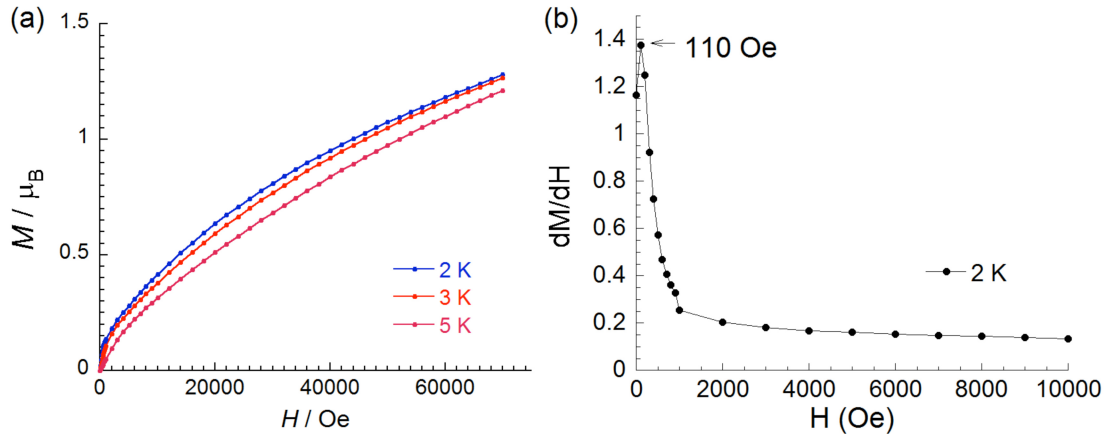

Figure 7. Magnetisation (*M*) *vs.* external magnetic field (*H*) for $(NMe_2H_2)_4[Cu_6O_2(SO_4)_6(DMF)_4]$ **1** (a) at the indicated temperatures and (b) its first derivative at 2 K showing an inflection point at a field of 110 Oe.

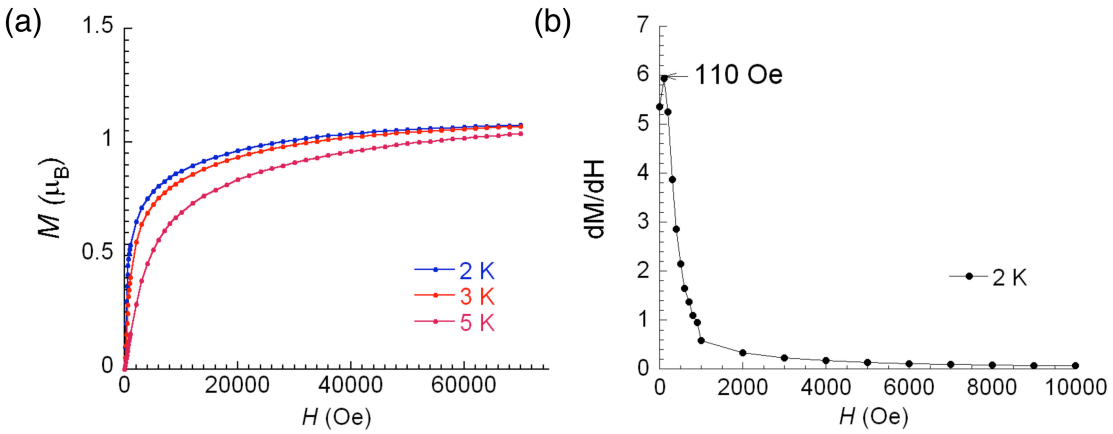

Figure 8. Magnetisation (*M*) *vs.* external magnetic field (*H*) for $(NMe_2H_2)[Cu(OH)(SO_4)_2(H_2O)_2]$ **3** (a) at the indicated temperatures and (b) its first derivative at 2 K showing an inflection point at a field of 110 Oe.

AC (alternating current) magnetic susceptibility studies, which monitor the response of a material's magnetic moment to an applied oscillating magnetic field, were also undertaken for the two compounds. The plots of the AC susceptibility in-phase (χ') component and out-of-phase (χ'') component for both **1** and **3** show the absence of χ'' (Fig. S5, S6) which is probably the result of the small canting angle. Therefore the magnetisation is almost cancelled when the spin carriers are antiferromagnetically coupled and only slightly canted. Canted antiferromagnetic behaviour has been observed previously in copper(II) compounds,[23,24] including the copper-hydroxy-sulfate mineral brochantite, $Cu_4(OH)_6SO_4$,[25] though metamagnetic behaviour is unusual.

Conclusions

We have prepared three new copper(II) sulfate compounds, in which the anionic charges on the copper-sulfate aggregates are balanced by the presence of dimethylammonium cations derived from either the decomposition of the DMF solvent or addition of $[NMe_2H_2]Cl$. Two of the new compounds, **1** and **2**, contain $Cu_6O_2(SO_4)_6$ aggregates, inter-connected by either hydrogen bonding or bridging sulfates, and the only previous report of these aggregates is in the rare copper sulfate mineral fedotovite. The third compound, **3**, has a tape structure in which triangular $Cu_3(OH)(SO_4)$ units share vertices. Magnetic measurements revealed that **1**

and **3** are both spin-canting metamagnetic systems, which is similar to the behaviour previously observed in some two- and three-dimensional copper(II)-containing networks.[23-26] Field-induced responses were observed below 5 K, with the critical field indicating metamagnetic behaviour from antiferromagnetic to ferromagnetic equal to 110 Oe for both compounds.

Associated content

Supporting information

Experimental and simulated powder X-ray diffraction patterns, magnetic measurements, hydrogen bonding distances and X-ray crystallographic files in CIF format of compounds **1-3**. This material is available free of charge via the Internet at http://pubs.acs.org.

Author information

Corresponding Author

*E-mail: a.d.burrows@bath.ac.uk. Tel.: +44-1225-386529. Fax: ++44-1225-386231.

Notes

The authors declare no competing financial interest.

Acknowledgements

The EPSRC is thanked for financial support.

References

(1) Jacobson, A. R.; Dousset, S.; Guichard, N.; Baveye, P.; Andreux, F. *Environ. Pollution* **2005**, *138*, 250.

(2) Reddy, A.; Ponder, E. L.; Fried, B. *J. Parasitol.* **2004**, *90*, 1332.

(3) Jančula, D.; Maršálek, B. *Chemosphere* **2011**, *85*, 1415.

(4) Wiese, J.; Harris, P.; Bradshaw, D. *Miner. Eng.* **2011**, *24*, 995.

(5) Pluth, J. J.; Steele, I. M.; Kampf, A. R.; Green, D. I. *Mineral. Mag.* **2005**, *69*, 973.

(6) Orlandi, P.; Bonaccorsi, E. *Can. Mineral.* **2009**, *47*, 143.

(7) Hawthorne, F. C.; Ferguson, R. B. *Acta Cryst. Sect. B* **1975**, *31*, 1753.

(8) Darling, K.; Ouellette, W.; Prosvirin, A.; Freund, S.; Dunbar, K. R.; Zubieta, J. *Cryst. Growth Des.* **2012**, *12*, 2662.

(9) Basu, C.; Biswas, S.; Chattopadhyay, A. P.; Stoeckli-Evans, H.; Mukherjee, S. *Eur. J. Inorg. Chem.* **2008**, 4927.

(10) Bacchi, A.; Carcelli, M.; Pelizzi, G.; Solinas, C.; Sorace, L. *Inorg. Chim. Acta* **2006**, *359*, 2275.

(11) Li, G.; Xing, Y.; Song, S.; Xu, N.; Liu, X.; Su, Z. *J. Solid State Chem.* **2008**, *181*, 2406.

(12) Lin, J.; Guo, D.-W.; Tian, Y.-Q. *Cryst. Growth Des.* **2008**, *8*, 4571.

(13) Burrows, A. D.; Cassar, K.; Friend, R. M. W.; Mahon, M. F.; Rigby, S. P.; Warren, J. E. *CrystEngComm* **2005**, *7*, 548.

(14) Kraus, W.; Nolzeb, G. *J. Appl. Cryst.* **1996**, *29*, 301.

(15) Sheldrick, G. *Acta Cryst. Sect. A* **2008**, *64*, 112.

(16) Vilminot, S.; Richard-Plouet, M.; André, G.; Swierczynski, D.; Guillot, M.; Bourée-Vigneron, F.; Drillon, M. *J. Solid State Chem.* **2003**, *170*, 255.

(17) Addison, A. W.; Rao, T. N.; Reedijk, J.; van Rijn, J.; Verschoor, G. C. *J. Chem. Soc., Dalton Trans.* **1984**, 1349.

(18) Starova, G. L.; Filatov, S. K.; Fundamensky, V. S.; Vergasova, L. P. *Mineral. Mag.* **1991**, *55*, 613.

(19) Ferrer, S.; Lloret, F.; Pardo, E.; Clemente-Juan, J. M.; Liu-González, M.; García-Granda, S. *Inorg. Chem.* **2012**, *51*, 985.

(20) Beckett, R.; Hoskins, B. F. *J. Chem. Soc., Dalton Trans.* **1972**, 291.

(21) Wu, J.; Hou, H.-W.; Guo, Y.-X.; Fan, Y.-T.; Wang, X. *Eur. J. Inorg. Chem.* **2009**, 2796.

(22) Pan, F.; Wu, J.; Hou, H.-W.; Fan, Y. *Cryst. Growth Des.* **2010**, *10*, 3835.

(23) Li, J.-R.; Yu, Q.; Sañudo, E. C.; Tao, Y.; Bu, X.-H. *Chem. Commun.* **2007**, 2602.

(24) Guo, L.-R.; Zhu, F.; Chen, Y.; Li, Y.-Z.; Zheng, L.-M. *Dalton Trans.* **2009**, 8548.

(25) Vilminot, S.; Richard-Plouet, M.; André, G.; Swierczynski, D.; Bourée-Vigneron, F.; Kurmoo, M. *Dalton Trans.* **2006**, 1455.

(26) Yang, E.-C.; Liu, Z.-Y.; Wu, X.-Y.; Chang, H.; Wang, E.-C.; Zhao, X.-J. *Dalton Trans.* **2011**, *40*, 10082.